Journal of Atomic, Molecular, Condensate & Nano Physics
Vol. 7, No. 2, pp. 115–131, 2020
ISSN 2349-2716 (online); 2349-6088 (print)
Published by RGN Publications

http://www.rgnpublications.com

DOI: 10.26713/jamcnp.v7i2.1455

Research Article

Energy Levels and Radiative Properties of Cu-like Tungsten

Ravinder Kumar[1,2], Sunny Aggarwal[2*] and Narendra Singh[1,2]

[1] *Department of Physics, Shyamlal College, University of Delhi, Delhi 110032, India*
[2] *Department of Physics & Astrophysics, University of Delhi, Delhi 110007, India*
***Corresponding author:** nsingh76@yahoo.co.in

Abstract. We have reported fine structure energies along with radiative data namely, transition wavelengths, transition probabilities, oscillator strengths and line strengths for lowest 120 levels of Cu-like W using *Multi-Configuration Dirac-Fock* (MCDF) method which may be useful ion for fusion plasma research. We have systematically analysed *configuration interaction* (CI) effects on Dirac-Coulomb as well as Breit and *Quantum electrodynamics* (QED) excitation energies and demonstrated that in order to attain accuracy in atomic data inclusions of CI in excitation energies are crucial. We have also discussed the evaluation of results from two independent codes GRASP and FAC. We have predicted some new energy levels and transition data where no other experimental or theoretical results are available. The present set of results should be useful in line identification and the interpretation of spectra, as well as in modeling of fusion plasmas.

Keywords. Oscillator strength; Radiative data; Correlation; Active set

PACS. 32.70.Cs

Received: August 13, 2020 **Accepted:** August 29, 2020

1. Introduction

Tungsten is of great interest for its intricate relationship with fusion plasma as many components of present and future generation tokamaks are made up of tungsten. The selection of tungsten as a plasma-facing material for the *International Thermonuclear Experimental Reactor* (ITER) has brought main interest in its spectroscopic studies [1]. A significant amount of energy may be released via the radiation emitted by the tungsten ions, as tungsten is usually

found as an impurity in the plasma [2]. The intermediate charge states of tungsten (including Cu-like W) are more prominent in plasmas with ion temperature of few KeV. The ions present in these charge states radiate a significant portion of their spectra in the *Extreme Ultraviolet* (EUV) region which has been investigated in the laser produced plasmas [3, 4]. The study of tungsten ions in the diagnosis and investigation of fusion as well as astrophysical plasma has significantly increased in past few decades [5–7]. Several experimental and theoretical methods have been used for determination of accurate atomic data for several ionization states of tungsten [8–11]. Recently, atomic structure on Li-like W to Yt-like W have been studied experimentally [12–15]. Impurity X-ray spectra for Cu-like W were measured at the ASDEX upgrade and JT600 tokamak [16]. In the theoretical approaches a significant improvement has been achieved in last few years in particular by the development of large-scale relativistic *configuration-interaction* (CI) methods taking into account electron correlation effects. An extended experimental and theoretical data based on tungsten ions can be found in refs. [17–19].

The study of ions along the Cu isoelectronic sequence provides important benchmark through both experiments and modern atomic structure theory. In the recent past, using several methods and techniques, various experimental and theoretical works on Cu-like ions have been performed, which has greatly shown the importance of Cu-like ions. Sansonetti *et al*. [20] provided the transition data with energy levels for Ba XXVIII and other Barium ions. Suzuki *et al*. [21] have observed EUV spectra for highly ionized Gd and Nd ions including Cu-like Gd and Nd by solid pellet injection in *Large Helical Device* (LHD) plasmas. Kilbane *et al*. [22] measured EUV spectra of Cu-like ions with flat-field grazing incidence. Goyal *et al*. [23] diagnose *extreme ultraviolet* (EUV) and *soft X-ray* (SXR) transitions with electron excitation to M-shell and higher shells in the theoretical study of Cu-like ions.

The atomic spectra of Cu-like W are not so well resolved and there is insufficiency of reliable and authentic atomic data for Cu-like tungsten due to the complex and complicated spectra of open N shells. Xu *et al*. [24] calculated excitation energies and wavelengths of nine isoelectronic sequence of tungsten ions (including Cu-like W) using MCDF method by taking into account the electron correlations, quantum electrodynamics effect (QED) and Breit corrections. Klapisch *et al*. [25] measured 3d-4p transitions in Cu-like tungsten(W) and Thulium(Tm) by classification of X-ray spectra from laser-produced plasmas. They also calculated [25] the transition wavelength and transition probabilities using relativistic parametric potential atomic structure code. Mandelbaum *et al*. [26] also studied the X-ray spectra from laser-produced plasma of Cu-like ions (including Cu-like W) using RELAC method. Klapisch *et al*. [27] studied the 3d-4f transitions in X-ray spectra of highly ionized Tm to Re. Zigler *et al*. [28] interpretate X-ray spectra in the 3 KeV range of Au and W. Recently, Rzadkiewicz *et al*. [29] measured the X-ray transitions in Cu and Ni like tungsten ions in the wavelength range of 5.19-5.26 Å. They [29] measured wavelength of ground state transitions in Cu-like tungsten from the $3p^5 3d^{10} 4s4p$ $[3/2,(1/2,5/2)_2]_{1/2}$ level. Fourier [17] studied the atomic data and spectral line intensities for highly charged tungsten ions in a tokamak plasma. Osberne *et al*. [30] reported spectroscopic analysis and modeling of tungsten EBIT and Z-pinch plasma experiments. Clementson *et al*. [31] investigate the spectroscopy of M-shell X-ray transitions in Zn-like through Co-like

tungsten. Ralchenko *et al*. [32] investigated the spectra of tungsten ions (Z = 39 to 47) in 12-20 nm region observed with EBIT. Palmeri *et al*. [33] calculated transition wavelengths and transition probabilities in Cu-like ions ($70 \leq Z \leq 92$). Safronova *et al*. [34] using the *relativistic many-body perturbation theory method* (RMBPT), the multiconfiguration relativistic *Hebrew University Lawrence Livermore Atomic Code* (HULLAC) and Hartree-Fock relativistic method (COWAN code) reported transition probabilities, energy levels and autoionization rates for some states in Cu-like tungsten. $4d$-$3p$ transitions in Cu-like tungsten ions have been studied by Kozial and Rzadkiewicz [35].

The aim of present paper is to upgrade the database of energy levels and radiative rates of Cu-like tungsten ion. We have reported the energy levels for 120 lowest levels. Further, we have presented the transition wavelength, transition probabilities, oscillator strength and line strength from ground state for electric dipole (E1), electric quadrupole (E2), magnetic dipole (M1) and magnetic quadrupole (M2) transitions. Since the investigations of highly charged Cu-like tungsten ion considered in present work require the simultaneous consideration of electronic correlation and relativistic effects therefore, we have used GRASP code which work on MCDF technology developed originally by Grant *et al*. [36] and revised by Norrington [37]. In our calculation, we have included the QED and Breit corrections which have been applied successfully to calculate atomic data for many highly charged ions [38–43]. In present calculations, all the orbitals were simultaneously optimized on the average energy of all configurations by using the option of EAL (extended average level).

We have structured this paper in the following way: in Section 2, we present the method of calculations, in Section 3, we present the result and discussion. Finally, we presented the conclusion in Section 4.

2. Method of Calculations

To execute these extensive calculations, we have adopted a fully relativistic MCDF method applied in *General purpose relativistic atomic structure package* (GRASP). This method was developed by Grant *et al*. [36] and improved by Norrington [37] and has been successfully applied in our previous works [38–43]. Since the elaborate explanation of this method has been presented in many papers, so we are not discussed it here.

For highly charged ions, the essential mechanism to attain reliability in the determination of atomic data is *configuration interaction* (CI). In last few years, the detailed analysis of configuration interaction on atomic data calculations has become popular. In order to assess the effect of configuration interaction on non relativistic energy and relativistic corrections, different sets are considered in the present work. In the first set, we have included the ground state configuration and other configuration from $n = 4$. In other sets, we have increased the orbitals in a systematic way and enhance the active set layer by layer. The division of levels in groups on the basis of parity and J values makes the computational procedure simple and manageable. In all sets, we have retained configurations of previous model. We have also included the contributions of Breit interactions and QED effects such as vacuum polarization and self-energy through *relativistic configuration interaction* (RCI) calculations. We enhanced

the size of the active set as shown below till $n = 7$. We have shown the effect of increasing principal quantum number on Breit, QED corrections and total energy in Table 1.

$AS1 = \{n = 4, l = 0 - 3\}$,

$AS2 = AS1 + \{n = 5, l = 0 - 4\}$,

$AS3 = AS2 + \{n = 6, l = 0 - 4\}$,

$AS4 = AS3 + \{n = 7, l = 0 - 4\}$.

Table 1. Energy (including Breit and QED) with increasing active set

$N = 4$				
Level number	DC	Breit	QED	Total
2	7.2219	8.05E-02	−7.45E-02	7.2279
3	14.7319	−9.89E-03	−6.60E-02	14.6560
4	25.8620	−3.53E-02	−7.37E-02	25.7529
5	27.4756	−7.24E-02	−7.37E-02	27.3295
6	39.3316	−1.05E-01	−7.37E-02	39.1531
7	39.7509	−1.29E-01	−7.37E-02	39.5482
$N = 5$				
Level number	DC	Breit	QED	Total
2	7.2293	8.05E-02	−7.58E-02	7.2339
3	14.7307	−9.77E-03	−6.71E-02	14.6538
4	25.7896	−6.03E-02	−7.50E-02	25.6543
5	27.4035	−9.78E-02	−7.50E-02	27.2307
6	39.3333	−1.04E-01	−7.50E-02	39.1538
7	39.7509	−1.29E-01	−7.50E-02	39.5472
$N = 6$				
Level number	DC	Breit	QED	Total
2	7.1996	6.10E-02	−7.58E-02	7.1848
3	14.7043	−3.03E-02	−6.71E-02	14.6069
4	25.7947	−5.93E-02	−7.50E-02	25.6604
5	27.4086	−9.68E-02	−7.50E-02	27.2368
6	39.3280	−1.05E-01	−7.50E-02	39.1484
7	39.7459	−1.29E-01	−7.50E-02	39.5421
$N = 7$				
Level number	DC	Breit	QED	Total
2	7.1735	5.45E-02	−7.64E-02	7.1516
3	14.6884	−3.58E-02	−6.76E-02	14.5850
4	25.8939	−3.21E-02	−7.56E-02	25.7861
5	27.5104	−7.00E-02	−7.56E-02	27.3647
6	39.3544	−1.05E-01	−7.56E-02	39.1740
7	39.7742	−1.29E-01	−7.56E-02	39.5701

3. Result and Discussion

Due to shortage of experimental measurements or theoretical data for higher excited states, production and comparison of atomic data such as energy levels and radiative rates from two or more independent codes has almost common in the theoretical atomic physics to assess accuracy and reliability of calculated data. Therefore, we have also calculated energy levels using *Flexible Atomic Code* (FAC) which is also fully relativistic and based on jj-coupling scheme.

In Table 2, we have reported the 120 fine structural energy values obtained using MCDF and FAC for Cu-like tungsten. Our final calculation includes $[1s^2 2s^2 2p^6 3s^2]3p^6 3d^{10} nl (n = 4-7, l = 0-4)$, $3p^6 3d^9 nl^2 (n = 4, l = 0-3)$, $3p^5 3d^{10} nl^2 (n = 4, l = 0-3)$, $3p^6 3d^9 nl n'l' (n, n' = 4-5, l, l' = 0-4)$ configurations. As QED and Breit correction are important for transition energy calculations, therefore we have presented the contributions of QED and Breit corrections calculated from MCDF method in Table 2. One can see from Table 2 that the contribution of Breit and QED corrections are significant for maximum levels therefore the contribution of QED and Breit corrections cannot be neglected for high Z ions. In Table 2, the column 'S.No.' indicates the level number of relativistic fine-structure levels listed under the second column 'configuration'. We have also tabulated the lifetimes of excited levels in Table 2. We have compared our calculated results of energy values from MCDF and FAC with the energy levels compiled by NIST, whose data are commonly used as reference set for atomic results. From the literature survey, it has been reviewed that the maximum discrepancy in energies calculated from the two different fully relativistic codes for the same configuration set cannot be more than 0.15 Ryd for highly charged ions and this discrepancy between two codes may be due to different ways of calculations of radial wavefunctions and different potential implemented in these codes.

In Table 2, our presented energy levels of MCDF are in good agreement with FAC and the maximum discrepancy between FAC and MCDF is 0.3% for $3p^6 3d^{10} 4d\ ^2D_{5/2}$. Small discrepancies between the energy calculated by using MCDF and FAC is mainly due to different ways of calculations of electron wave-functions for radial orbits and recoupling scheme of angular parts for all levels, whose data was present in NIST database. Our calculated energy values are in good agreement with the NIST values (maximum discrepancy 0.35%) which confirm the credibility and integrity of our results. Further, we would like to mention that we have reported results for many new energy levels, which are not listed in the NIST tables. Higher levels corresponding to $3p^6 3d^9 4p^2$ and many from $3p^6 3d^9 4s4p$ are obtained for the first time.

In Table 3, we have compared calculated results of energy levels from MCDF and FAC with the calculated values of Safronova *et al*. [34] which also used two independent methods for their calculations. We have also presented the % difference in energies of different calculations with NIST as well as from each other. For the level $3p^6 3d^{10} 4p$, the results of Safronova *et al*. [34] calculated from Cowan's code differ from all other results. Our calculated values from MCDF method for all transitions match well with the calculated values of Safronova *et al*. [34] using RMBPT code as well as with the data compiled by NIST. The maximum difference between two calculations is 0.33%. This is a clear indication of accuracy of our results as this is a criterian to judge reliability of theoretical results.

Table 2. Dirac-Coulomb (DC), Breit, and Quantum electrodynamics (QED) contributions to the MCDF energy (in Rydberg) as a function of the orbital set. The sum (Total) is compared with FAC and NIST. All energies are relative to the ground state

S. No.	Configuration	Term	J	Lifetime	MCDF				FAC	NIST
					DC	Breit	QED	Total		
1	$3P^6 3D^{10} 4S$	^2S	1/2	—	—	—	—	—	0.0000	0.0000
2	$3P^6 3D^{10} 4P$	^2P	1/2	2.12E-11	7.1735	0.0545	-0.0764	7.15162	7.1407	7.1754
3	$3P^6 3D^{10} 4P$	^2P	3/2	2.39E-12	14.6884	-0.0358	-0.0676	14.585	14.5934	14.6186
4	$3P^6 3D^{10} 4D$	^2D	3/2	1.16E-12	25.8939	-0.0321	-0.0756	25.7861	25.7100	25.6940
5	$3P^6 3D^{10} 4D$	^2D	5/2	2.98E-12	27.5104	-0.07	-0.0756	27.3647	27.2923	27.2792
6	$3P^6 3D^{10} 4F$	^2F	5/2	3.36E-12	39.3544	-0.105	-0.0756	39.174	39.1283	39.1240
7	$3P^6 3D^{10} 4F$	^2F	7/2	4.31E-12	39.7742	-0.129	-0.0756	39.5701	39.5261	39.5230
8	$3P^6 3D^{10} 5S$	^2S	1/2	1.01E-13	71.2125	-0.083	-0.0444	71.0851	71.0680	71.12
9	$3P^6 3D^{10} 5P$	^2P	1/2	1.17E-13	74.7169	-0.0437	-0.0763	74.5969	74.5516	74.60
10	$3P^6 3D^{10} 5P$	^2P	3/2	1.79E-13	78.2424	-0.0851	-0.0723	78.085	78.0485	78.10
11	$3P^6 3D^{10} 5D$	^2D	3/2	1.62E-13	83.5788	-0.0888	-0.0756	83.4145	83.3355	83.51
12	$3P^6 3D^{10} 5D$	^2D	5/2	1.41E-13	84.3629	-0.108	-0.0756	84.1791	84.1021	84.16
13	$3P^6 3D^{10} 5F$	^2F	5/2	8.71E-14	89.6102	-0.131	-0.0756	89.4036	89.3547	89.42
14	$3P^6 3D^{10} 5F$	^2F	7/2	8.57E-14	89.8503	-0.141	-0.0756	89.6333	89.5863	89.65
15	$3P^6 3D^{10} 5G$	^2G	7/2	4.80E-14	92.497	-0.151	-0.0756	92.2702	92.2600	92.32
16	$3P^6 3D^{10} 5G$	^2G	9/2	4.83E-14	92.593	-0.153	-0.0756	92.364	92.3533	92.41
17	$3P^6 3D^{10} 6S$	^2S	1/2	1.15E-13	106.798	-0.0808	-0.0603	106.657	106.5520	
18	$3P^6 3D^{10} 6P$	^2P	1/2	1.29E-13	108.747	-0.0597	-0.076	108.611	108.4980	
19	$3P^6 3D^{10} 6P$	^2P	3/2	1.88E-13	110.686	-0.0814	-0.074	110.531	110.4400	
20	$3P^6 3D^9 4S^2$	^2D	5/2	1.64E-10	113.614	-0.128	0.0746	113.561	113.3813	113.74
21	$3P^6 3D^{10} 6D$	^2D	3/2	1.69E-13	113.631	-0.0869	-0.0756	113.468	113.7218	
22	$3P^6 3D^{10} 6D$	^2D	5/2	1.50E-13	114.072	-0.0975	-0.0756	113.899	113.8231	
23	$3P^6 3D^{10} 6F$	^2F	5/2	1.01E-13	116.925	-0.106	-0.0756	116.744	116.685	116.67
24	$3P^6 3D^{10} 6F$	^2F	7/2	1.01E-13	117.068	-0.111	-0.0756	116.881	116.8299	116.79
25	$3P^6 3D^9 4S^2$	^2D	3/2	7.77E-14	118.55	-0.117	-0.0756	118.358	118.307	
26	$3P^6 3D^{10} 6G$	^2G	7/2	5.81E-11	118.562	-0.233	0.0747	118.404	118.3636	118.29
27	$3P^6 3D^{10} 6G$	^2G	9/2	7.82E-14	118.607	-0.119	-0.0756	118.413	118.5875	118.30
28	$3P^6 3D^9 4S4P$	^4P	5/2	1.53E-09	119.841	-0.042	-0.00079	119.798	119.9114	
29	$3P^6 3D^9 4S4P$	^4F	7/2	5.70E-11	120.394	-0.0562	-0.000788	120.337	120.4499	
30	$3P^6 3D^9 4S4P$	^2F	5/2	6.49E-11	120.395	-0.0475	-0.000748	120.347	120.4625	
31	$3P^6 3D^9 4S4P$	^2P	3/2	3.47E-11	120.452	-0.0365	-0.000763	120.415	120.5299	
32	$3P^6 3D^9 4S4P$	^4F	3/2	1.03E-12	124.823	-0.151	-0.000762	124.672	124.8082	124.92
33	$3P^6 3D^9 4S4P$	^4F	5/2	4.71E-11	125.36	-0.16	-0.000746	125.199	125.3351	
34	$3P^6 3D^{10} 4S4P$	^4P	3/2	1.73E-13	125.444	-0.151	-0.000706	125.292	125.4337	125.48
35	$3P^6 3D^9 4S4P$	^4D	1/2	1.63E-13	125.519	-0.145	-0.000715	125.373	125.5141	125.48
36	$3P^6 3D^{10} 7S$	^2S	1/2	1.47E-13	127.065	-0.0965	-0.0667	126.902	126.836	
37	$3P^6 3D^9 4S4P$	^4F	9/2	2.19E-07	127.317	-0.148	0.00789	127.176	127.3026	

Contd. Table 2

S. No.	Configuration	Term	J	Lifetime	MCDF				FAC	NIST
					DC	Breit	QED	Total		
38	$3P^6 3D^9 4P4P$	^2D	5/2	1.15E-10	127.591	-0.134	0.00782	127.465	127.5976	
39	$3P^6 3D^9 4S4P$	^4D	3/2	2.11E-13	127.599	-0.132	0.0078	127.474	127.6129	127.68
40	$3P^6 3D^9 4S4P$	^4D	7/2	4.56E-10	127.655	-0.138	0.00788	127.524	127.6586	
41	$3P^6 3D^9 4S4P$	^2P	1/2	8.85E-14	127.671	-0.132	0.0077	127.547	127.6945	127.79
42	$3P^6 3D^9 4P^2$	^2D	5/2	8.11E-12	128.061	0.0369	-0.0764	128.021	128.0280	
43	$3P^6 3D^{10} 7P$	^2P	1/2	1.49E-13	128.258	-0.0835	-0.0758	128.099	128.0896	
44	$3P^6 3D^9 4S4P$	^2P	3/2	1.23E-13	128.755	-0.135	0.00747	128.627	128.7593	128.76
45	$3P^6 3D^9 4S4P$	^2F	7/2	1.47E-12	128.768	-0.142	0.00744	128.633	128.7596	
46	$3P^6 3D^9 4S4P$	^2D	5/2	1.42E-12	129.006	-0.134	0.00736	128.88	129.0108	
47	$3P^6 3D^{10} 7P$	^2P	3/2	2.01E-13	129.44	-0.0966	-0.0744	129.269	129.2123	
48	$3P^6 3D^{10} 7D$	^2D	3/2	1.99E-13	131.239	-0.0997	-0.0756	131.064	131.0080	
49	$3P^6 3D^{10} 7D$	^2D	5/2	1.80E-13	131.512	-0.106	-0.0756	131.33	131.2810	
50	$3P^6 3D^9 4S4P$	^4P	1/2	2.41E-12	132.136	-0.228	0.00785	131.916	132.0638	132.14
51	$3P^6 3D^9 4S4P$	^4D	3/2	8.75E-13	132.421	-0.236	0.00787	132.192	132.3464	132.37
52	$3P^6 3D^9 4S4P$	^2F	7/2	3.39E-10	132.462	-0.253	0.00789	132.217	132.3729	
53	$3P^6 3D^9 4S4P$	^4D	5/2	1.84E-10	132.573	-0.241	0.00788	132.34	132.4958	
54	$3P^6 3D^9 4P^2$	^4F	3/2	2.10E-13	133.095	-0.0713	-0.0764	132.948	133.0168	133.01
55	$3P^6 3D^{10} 7F$	^2F	5/2	1.31E-13	133.242	-0.111	-0.0756	133.055	133.0416	
56	$3P^6 3D^{10} 7F$	^2F	7/2	1.31E-13	133.333	-0.114	-0.0756	133.143	133.1091	
57	$3P^6 3D^9 4S4P$	^2P	1/2	4.03E-13	133.592	-0.237	0.00764	133.362	133.5113	133.48
58	$3P^6 3D^9 4S4P$	^2F	5/2	1.45E-12	133.758	-0.246	0.00747	133.519	133.6697	
59	$3P^6 3D^9 4S4P$	^2D	3/2	6.60E-13	133.906	-0.238	0.00742	133.675	133.8272	
60	$3P^6 3D^{10} 7G$	^2G	7/2	5.95E-14	134.249	-0.118	-0.0756	134.056	134.0170	
61	$3P^6 3D^{10} 7G$	^2G	9/2	6.00E-14	134.285	-0.119	-0.0756	134.091	134.0530	
62	$3P^6 3D^9 4P^2$	^4D	7/2	1.00E-12	135.053	-0.0553	-0.0681	134.93	135.0111	
63	$3P^6 3D^9 4P^2$	^2G	9/2	1.75E-12	135.2	-0.0773	-0.0651	135.058	135.1419	
64	$3P^6 3D^9 4P^2$	^2P	3/2	7.86E-13	135.232	-0.0487	-0.0668	135.116	135.2008	
65	$3P^6 3D^9 4P^2$	^2F	5/2	1.18E-12	135.296	-0.0596	-0.067	135.169	135.2559	
66	$3P^6 3D^9 4P^2$	^2S	1/2	5.28E-14	135.332	-0.0509	-0.0645	135.216	135.3117	
67	$3P^6 3D^9 4P^2$	^2D	3/2	4.54E-14	135.371	-0.0578	-0.0667	135.247	135.3461	
68	$3P^6 3D^9 4P^2$	^4P	5/2	1.16E-12	135.432	-0.0482	-0.0668	135.317	135.4061	
69	$3P^6 3D^9 4P^2$	^4F	7/2	2.90E-12	135.529	-0.0646	-0.0657	135.398	135.4895	
70	$3P^6 3D^9 4P^2$	^4D	1/2	1.09E-12	138.695	-0.149	-0.0003	138.546	138.6257	
71	$3P^6 3D^9 4P^2$	^2G	7/2	1.09E-12	139.044	-0.172	-4.5E-05	138.872	139.0507	
72	$3P^6 3D^9 4P^2$	^4F	3/2	1.05E-12	139.111	-0.159	-0.00029	138.952	139.1029	
73	$3P^6 3D^9 4P^2$	^4F	5/2	7.14E-13	139.173	-0.14	-0.00348	139.03	139.1145	
74	$3P^6 3D^9 4P^2$	^2P	1/2	9.86E-13	139.212	-0.18	-0.00193	139.03	139.2025	
75	$3P^6 3D^9 4P^2$	^2F	5/2	8.91E-13	139.382	-0.156	-0.00151	139.224	139.3696	
76	$3P^6 3D^9 4P^2$	^2D	3/2	9.79E-13	139.434	-0.165	-0.00192	139.267	139.4487	
77	$3P^6 3D^9 4P^2$	^4F	9/2	9.34E-13	139.49	-0.158	-0.00144	139.33	139.5086	

Contd. Table 2

S. No.	Configuration	Term	J	Lifetime	MCDF				FAC	NIST
					DC	Breit	QED	Total		
78	$3P^6 3D^9 4P^2$	^2F	7/2	8.55E-13	139.845	-0.152	-0.0668	139.626	139.7846	
79	$3P^6 3D^9 4P^2$	^2P	1/2	5.62E-13	140.139	-0.162	-0.0674	139.91	140.0888	
80	$3P^6 3D^9 4P^2$	^2D	5/2	3.49E-12	140.176	-0.18	-0.0649	139.931	140.1243	
81	$3P^6 3D^9 4P^2$	^2P	3/2	4.07E-13	140.233	-0.165	-0.0682	140	140.1909	140.05
82	$3P^6 3D^9 4S(^3D)4D$	^4S	3/2	1.34E-13	140.297	-0.158	-0.0649	140.074	140.262	
83	$3P^6 3D^9 4P^2$	^2D	5/2	2.85E-12	140.452	-0.221	-7.8E-05	140.231	140.4079	
84	$3P^6 3D^9 4S(^3D)4D$	^4G	7/2	2.17E-13	140.46	-0.167	-0.0654	140.228	140.4234	
85	$3P^6 3D^9 4S(^3D)4D$	^4D	5/2	2.52E-13	140.523	-0.166	-0.058	140.299	140.491	140.34
86	$3P^6 3D^9 4S(^3D)4D$	^4G	9/2	3.08E-13	140.593	-0.192	-0.0089	140.392	140.5418	
87	$3P^6 3D^9 4S(^1D)4D$	^2P	1/2	1.11E-12	140.699	-0.201	-0.00377	140.495	140.6366	
88	$3P^6 3D^9 4S(^3D)4D$	^4D	3/2	2.73E-12	140.804	-0.2	-0.00047	140.603	140.7753	
89	$3P^6 3D^9 4S(^3D)4D$	^4D	7/2	2.71E-12	140.861	-0.205	-0.00035	140.656	140.8424	
90	$3P^6 3D^9 4S(^3D)4D$	^4G	11/2	2.46E-12	140.882	-0.19	-1E-04	140.691	140.8684	
91	$3P^6 3D^9 4S(^1D)4D$	^2F	5/2	2.73E-12	141.053	-0.202	-0.0092	140.842	141.0286	
92	$3P^6 3D^9 4P^2$	^4P	3/2	8.31E-13	141.243	-0.18	-0.00769	141.055	141.2387	
93	$3P^6 3D^9 4P^2$	^4P	1/2	6.06E-13	141.261	-0.185	-0.00929	141.066	141.2393	
94	$3P^6 3D^9 4P^2$	^2F	7/2	2.93E-12	141.314	-0.188	-0.0115	141.114	141.2923	
95	$3P^6 3D^9 4P^2$	^4D	5/2	5.70E-13	142.136	-0.186	-0.00979	141.94	142.0962	
96	$3P^6 3D^9 4S(^1D)4D$	^2D	3/2	9.08E-13	143.279	-0.163	-0.052	143.064	143.2267	
97	$3P^6 3D^9 4S(^1D)4D$	^2F	7/2	3.58E-13	143.336	-0.152	-0.0487	143.136	143.2458	
98	$3P^6 3D^9 4S(^3D)4D$	^4F	9/2	8.79E-13	143.365	-0.157	-0.0494	143.158	143.324	
99	$3P^6 3D^9 4S(^1D)4D$	^2D	5/2	9.83E-14	143.484	-0.152	-0.0538	143.278	143.4184	
100	$3P^6 3D^9 4S(^1D)4D$	^2S	1/2	1.14E-13	143.535	-0.146	-0.0532	143.336	143.4806	
101	$3P^6 3D^9 4S(^3D)4D$	^4P	1/2	1.07E-12	143.871	-0.276	-0.0002	143.595	143.7988	
102	$3P^6 3D^9 4P^2$	^2D	3/2	1.01E-12	143.909	-0.143	-0.0579	143.708	143.8957	143.42
103	$3P^6 3D^9 4S(^3D)4D$	^2G	9/2	9.43E-13	144.013	-0.269	-0.00124	143.743	143.9218	
104	$3P^6 3D^9 4S(^3D)4D$	^2P	3/2	9.56E-13	144.07	-0.274	-0.00095	143.796	143.9779	
105	$3P^6 3D^9 4S(^3D)4D$	^4G	5/2	9.77E-13	144.208	-0.284	-0.00193	143.922	144.1297	
106	$3P^6 3D^9 4S(^3D)4D$	^2D	5/2	9.69E-13	144.352	-0.261	-0.001	144.09	144.2949	
107	$3P^6 3D^9 4S(^1D)4D$	^2P	3/2	8.49E-13	144.541	-0.268	-0.00174	144.272	144.4856	
108	$3P^6 3D^9 4S(^3D)4D$	^4D	1/2	1.41E-11	145.239	-0.0552	-0.076	145.108	145.2355	
109	$3P^6 3D^9 4S(^3D)4D$	^2F	7/2	2.71E-12	145.346	-0.286	-0.00019	145.06	145.2418	
110	$3P^6 3D^9 4S(^1D)4D$	^2G	7/2	1.08E-11	145.458	-0.0632	-0.076	145.319	145.4536	
111	$3P^6 3D^9 4S(^3D)4D$	^2D	5/2	2.77E-12	145.607	-0.323	-7.1E-05	145.284	145.4995	
112	$3P^6 3D^9 4S(^3D)4D$	^4P	3/2	1.49E-11	145.625	-0.101	-0.076	145.448	145.5879	
113	$3P^6 3D^9 4S(^3D)4D$	^4F	5/2	2.71E-12	145.685	-0.3	-7.8E-05	145.385	145.5996	
114	$3P^6 3D^9 4S(^1D)4D$	^2G	9/2	1.37E-11	145.732	-0.0729	-0.076	145.583	145.6961	
115	$3P^6 3D^9 4S(^3D)4D$	^4P	5/2	2.68E-12	145.792	-0.306	-0.00094	145.486	145.7229	
116	$3P^6 3D^9 4S(^3D)4D$	^4F	7/2	1.18E-11	145.804	-0.0818	-0.0761	145.646	145.7229	
117	$3P^6 3D^9 4S(^3D)4D$	^2P	1/2	2.27E-12	145.818	-0.279	-0.00652	145.532	145.7887	
118	$3P^6 3D^9 4S(^3D)4D$	^2G	7/2	2.75E-12	146.071	-0.305	-0.00836	145.758	145.9727	
119	$3P^6 3D^9 4S(^3D)4D$	^2D	3/2	2.18E-12	146.125	-0.287	-0.0109	145.827	146.0342	
120	$3P^6 3D^9 4S(^3D)4D$	^2F	5/2	1.18E-12	146.239	-0.291	-0.011	145.937	146.1436	

Table 3. Energy level (in Rydberg) for the some levels compared with other available results

Configuration	Term	J	cowan[a]	RMBPT[a]	GRASP(cal.)	FAC (cal.)	NIST	C-G	R-G	C-N	R-N	G-N
$3P^6 3D^{10} 4P$	^2P	1/2	7.0441	7.1753	7.171	7.14	7.1754	-1.8015	0.0599	-1.8639	-0.0013	-0.06136
$3P^6 3D^{10} 4P$	^2P	3/2	14.748	14.634	14.585	14.593	14.619	1.1052	0.3348	0.8746	0.1025	-0.2331
$3P^6 3D^{10} 4D$	^2D	3/2	25.552	25.7	25.786	25.71	25.694	-0.9157	-0.3346	-0.5557	0.0233	0.3567
$3P^6 3D^{10} 4D$	^2D	5/2	27.186	27.286	27.364	27.292	27.279	-0.6547	-0.2858	-0.3420	0.0256	0.3106
$3P^6 3D^{10} 4F$	^2F	5/2	38.997	39.127	39.174	39.128	39.124	-0.4538	-0.1201	-0.3256	0.0076	0.1276
$3P^6 3D^{10} 4F$	^2F	7/2	39.456	39.529	39.570	39.526	39.523	-0.2889	-0.1037	-0.1698	0.0151	0.1187
$3P^6 3D^{10} 5S$	^2S	1/2	71.086	71.115	71.085	71.068	71.12	0.0014	0.0421	-0.0478	-0.0070	-0.0492
$3P^6 3D^{10} 5P$	^2P	1/2	74.491	74.604	74.596	74.552	74.6	-0.1409	0.0107	-0.1463	0.0053	-0.0053
$3P^6 3D^{10} 5P$	^2P	3/2	78.135	78.105	78.085	78.049	78.1	0.0639	0.0256	0.0447	0.0064	-0.0192
$3P^6 3D^{10} 5D$	^2D	3/2	83.277	83.383	83.414	83.336	83.51	-0.1645	-0.0371	-0.2797	-0.1523	-0.1150
$3P^6 3D^{10} 5D$	^2D	5/2	84.072	84.152	84.179	84.102	84.16	-0.1272	-0.0320	-0.1046	-0.0095	0.0225
$3P^6 3D^{10} 5F$	^2F	5/2	89.314	89.415	89.403	89.355	89.42	-0.0996	0.0134	-0.1186	-0.0055	-0.0190
$3P^6 3D^{10} 5F$	^2F	7/2	89.558	89.648	89.633	89.586	89.65	-0.0837	0.0167	-0.1027	-0.0022	-0.0189
$3P^6 3D^{10} 5G$	^2G	7/2	92.212	92.319	92.270	92.26	92.32	-0.0629	0.0530	-0.1171	-0.0010	-0.0541
$3P^6 3D^{10} 5G$	^2G	9/2	92.312	92.413	92.364	92.353	92.41	-0.0563	0.0530	-0.1061	0.0032	-0.0498
$3P^6 3D^{10} 6S$	^2S	1/2	106.53	106.57	106.65	106.55		-0.1126	-0.0750			
$3P^6 3D^{10} 6P$	^2P	1/2	108.42	108.51	108.61	108.5		-0.1752	-0.0921			
$3P^6 3D^{10} 6P$	^2P	3/2	110.43	110.44	110.53	110.44		-0.0905	-0.0814			
$3P^6 3D^9 4S^2$	^2D	5/2	113.28	113.37	113.56	113.38	113.74	-0.2471	-0.1675	-0.4060	-0.3263	-0.1585
$3P^6 3D^{10} 6D$	^2D	3/2	113.73	113.8	113.46	113.72		0.2374	0.2987			
$3P^6 3D^{10} 6F$	^2F	5/2	116.57	116.65	116.74	116.69	116.67	-0.1458	-0.0771	-0.0857	-0.0171	0.0599
$3P^6 3D^{10} 6F$	^2F	7/2	116.71	116.79	116.88	116.83	116.79	-0.1456	-0.0770	-0.0685		0.0770
$3P^6 3D^9 4S^2$	^2D	3/2	118.21	118.29	118.35	118.31		-0.1184	-0.0507			
$3P^6 3D^{10} 6G$	^2G	7/2	118.27	118.35	118.40	118.36	118.29	-0.1099	-0.0422	-0.0169	0.0506	0.0929

a — Ref. [34]
C-G = %diff. between Cowan [34] and GRASP
R-G = %diff. between RMBPT [34] and GRASP
C-N = %diff. between Cowan [34] and NIST
R-N = %diff. between RMBPT [34] and NIST
G-N = %diff. between NIST and GRASP

In Table 4, we have presented transition wavelength, oscillator strength, transition probabilities and line strength for E1, E2, M1, M2 transition from the ground state in the length form alone, because for weaker transitions the negative energy states contribute to the velocity gauge [44] whereas the length gauge is relatively least affected. The basic principle to measure the accuracy of our presented results is the agreement between velocity and length. Therefore, vel./len. Ratios of oscillator strength are provided in the last column of Table 4. In many strong transitions, ratio is very near to one but the ratio is way from unity for weaker transitions integrals. One can see from Table 4, for all strong transitions the difference in ratio of len./vel. Form is maximum 10%.

Table 4. Transition data for E1, E2, M1 and M2 transitions from ground level, wavelength λ (in Å), line strength S (length form), oscillator strength f (length form), transition rate A_{ji} (length form) calculated using MCDF. Wavelngth are also compared with NIST

Transition		λ (Å)	λ (Å)	$A_{ij}(s^{-1})$	F_{ij}	S_{ji} (a.u)	vel/len	Transitions
I	J	(GRASP)	(NIST)					type
1	2	1.27E+02	126.998	4.72E+10	1.15E-01	9.64E-02	1.00E+00	E1
1	3	6.25E+01	62.336	4.19E+11	4.90E-01 4.93E-01[h] 4.82E-01[h]	2.02E-01	1.00E+00	E1
1	9	1.22E+01	12.216	4.65E+12	1.04E-01	8.36E-03	9.90E-01	E1
1	10	1.17E+01	11.675	2.48E+12	1.01E-01	7.77E-03	9.90E-01	E1
1	18	8.39E+00		2.98E+12	3.15E-02	1.74E-03	9.70E-01	E1
1	19	8.24E+00		1.84E+12	3.75E-02	2.04E-03	9.80E-01	E1
1	31	7.57E+00		9.78E+09	1.68E-04	8.37E-06	6.70E-01	E1
1	32	7.31E+00	7.295	9.72E+11	1.56E-02	7.49E-04	9.20E-01	E1
1	34	7.27E+00	7.262	5.77E+12	9.15E-02	4.38E-03	9.20E-01	E1
1	35	7.27E+00	7.262	6.12E+12	4.84E-02	2.32E-03	9.30E-01	E1
1	39	7.15E+00	7.137	4.73E+12	7.25E-02	3.41E-03	9.20E-01	E1
1	41	7.14E+00	7.131	1.13E+13	8.64E-02	4.07E-03	9.20E-01	E1
1	43	7.11E+00		2.52E+12	1.91E-02	8.96E-04	9.00E-01	E1
1	44	7.08E+00	7.077	7.47E+12	1.12E-01	5.24E-03	9.40E-01	E1
1	47	7.05E+00		1.89E+12	2.82E-02	1.31E-03	8.70E-01	E1
1	50	6.91E+00	6.896	4.11E+11	2.94E-03	1.34E-04	9.10E-01	E1
1	51	6.89E+00	6.884	1.14E+12	1.63E-02	7.39E-04	9.10E-01	E1
1	57	6.83E+00	6.827	1.85E+12	1.30E-02	5.83E-04	9.40E-01	E1
1	59	6.82E+00		5.52E+10	7.70E-04	3.45E-05	8.60E-01	E1
1	59	6.82E+00		5.52E+10	7.70E-04	3.45E-05	8.60E-01	E1
1	108	6.28E+00		6.49E+09	3.84E-05	1.59E-06	1.20E+00	E1
1	110	6.27E+00		3.79E+09	4.47E-05	1.85E-06	1.00E+00	E1
1	4	3.53E+01		4.89E+02	1.83E-10	3.20E-06		M1
1	8	1.28E+01		2.21E+05	5.45E-09	3.45E-05		M1
1	11	1.09E+01		2.84E+00	1.02E-13	5.49E-10		M1
1	17	8.54E+00		3.13E+05	3.42E-09	1.45E-05		M1
1	21	8.03E+00		2.12E+02	4.09E-12	1.62E-08		M1
1	26	7.70E+00		2.19E+03	3.89E-11	1.48E-07		M1
1	36	7.18E+00		2.47E+05	1.91E-09	6.78E-06		M1
1	48	6.95E+00		3.67E+01	5.31E-13	1.83E-09		M1
1	54	6.85E+00		3.43E+02	4.84E-12	1.64E-08		M1
1	64	6.74E+00		9.22E+03	1.26E-10	4.20E-07		M1
1	66	6.74E+00		3.07E+06	2.09E-08	6.97E-05		M1
1	67	6.74E+00		1.47E+04	2.00E-10	6.67E-07		M1
1	64	6.74E+00		9.22E+03	1.26E-10	4.20E-07		M1
1	66	6.74E+00		3.07E+06	2.09E-08	6.97E-05		M1
1	67	6.74E+00		1.47E+04	2.00E-10	6.67E-07		M1

Contd. Table 4

Transition		λ (Å)	λ (Å)	$A_{ij}(s^{-1})$	F_{ij}	S_{ji} (a.u)	vel/len	Transitions
I	J	(GRASP)	(NIST)					type
1	70	6.58E+00		4.17E+07	5.41E-07	1.76E-03		M1
1	73	6.55E+00		2.61E+07	1.68E-07	5.44E-04		M1
1	75	6.55E+00		6.13E+06	7.88E-08	2.55E-04		M1
1	78	6.53E+00		2.57E+05	1.64E-09	5.29E-06		M1
1	79	6.51E+00		2.56E+04	3.26E-10	1.05E-06		M1
1	82	6.51E+00		1.05E+06	6.68E-09	2.15E-05		M1
1	85	6.50E+00		4.95E+06	6.26E-08	2.01E-04		M1
1	86	6.49E+00		1.04E+07	1.31E-07	4.22E-04		M1
1	87	6.49E+00		3.36E+07	2.12E-07	6.79E-04		M1
1	92	6.46E+00		6.63E+05	8.30E-09	2.65E-05		M1
1	95	6.42E+00		6.53E+04	4.03E-10	1.28E-06		M1
1	97	6.37E+00		2.09E+06	1.27E-08	4.00E-05		M1
1	100	6.36E+00		1.19E+05	1.44E-09	4.52E-06		M1
1	103	6.34E+00		7.48E+06	4.51E-08	1.41E-04		M1
1	104	6.34E+00		1.44E+07	1.74E-07	5.45E-04		M1
1	106	6.32E+00		1.65E+06	1.97E-08	6.18E-05		M1
1	109	6.28E+00		1.90E+07	2.25E-07	7.00E-04		M1
1	117	6.26E+00		2.36E+07	1.39E-07	4.29E-04		M1
1	119	6.25E+00		7.68E+05	8.99E-09	2.78E-05		M1
1	4	3.53E+01		1.21E+08	4.55E-05	2.39E-02	1.00E+00	E2
1	5	3.33E+01		1.67E+08	8.34E-05	3.67E-02	1.00E+00	E2
1	11	1.09E+01		1.15E+10	4.12E-04	6.40E-03	9.90E-01	E2
1	12	1.08E+01		1.09E+10	5.75E-04	8.69E-03	9.90E-01	E2
1	20	8.02E+00		4.67E+09	1.35E-04	8.33E-04	9.10E-01	E2
1	21	8.03E+00		8.67E+09	1.68E-04	1.03E-03	9.50E-01	E2
1	22	8.00E+00		8.65E+09	2.49E-04	1.52E-03	9.50E-01	E2
1	26	7.70E+00		5.15E+09	9.15E-05	4.97E-04	9.10E-01	E2
1	42	7.12E+00		2.70E+07	6.16E-07	2.65E-06	8.00E-01	E2
1	48	6.95E+00		7.98E+09	1.16E-04	4.63E-04	6.80E-01	E2
1	49	6.94E+00		8.01E+09	1.73E-04	6.90E-04	6.70E-01	E2
1	54	6.85E+00		2.78E+07	3.91E-07	1.50E-06	1.20E+00	E2
1	64	6.74E+00		1.97E+07	2.69E-07	9.84E-07	1.30E+00	E2
1	65	6.74E+00		1.55E+08	3.16E-06	1.15E-05	1.10E+00	E2
1	67	6.74E+00		2.07E+07	2.81E-07	1.03E-06	4.90E-01	E2
1	68	6.73E+00		1.67E+08	3.41E-06	1.24E-05	1.10E+00	E2
1	64	6.74E+00		1.97E+07	2.69E-07	9.84E-07	1.30E+00	E2
1	65	6.74E+00		1.55E+08	3.16E-06	1.15E-05	1.10E+00	E2
1	67	6.74E+00		2.07E+07	2.81E-07	1.03E-06	4.90E-01	E2
1	68	6.73E+00		1.67E+08	3.41E-06	1.24E-05	1.10E+00	E2
1	70	6.58E+00		1.00E+08	1.30E-06	4.41E-06	9.70E-01	E2
1	72	6.56E+00		2.15E+09	4.16E-05	1.40E-04	9.60E-01	E2
1	75	6.55E+00		6.42E+09	8.24E-05	2.75E-04	9.50E-01	E2
1	77	6.54E+00		1.23E+08	2.37E-06	7.89E-06	9.40E-01	E2

Contd. Table 4

Transition		λ (Å)	λ (Å)	$A_{ij}(s^{-1})$	F_{ij}	S_{ji} (a.u)	vel/len	Transitions
I	J	(GRASP)	(NIST)					type
1	79	6.51E+00		1.08E+08	1.38E-06	4.54E-06	9.60E-01	E2
1	81	6.51E+00		9.24E+06	1.76E-07	5.79E-07	1.70E+00	E2
1	84	6.50E+00		8.05E+07	1.53E-06	5.00E-06	8.30E-01	E2
1	85	6.50E+00		3.28E+08	4.15E-06	1.35E-05	9.40E-01	E2
1	86	6.49E+00		4.06E+09	5.13E-05	1.67E-04	9.50E-01	E2
1	90	6.48E+00		1.64E+10	3.09E-04	1.00E-03	9.60E-01	E2
1	92	6.46E+00		1.54E+10	1.93E-04	6.18E-04	9.70E-01	E2
1	93	6.46E+00		6.60E+09	1.24E-04	3.98E-04	9.50E-01	E2
1	99	6.36E+00		7.31E+08	1.33E-05	4.08E-05	1.00E+00	E2
1	100	6.36E+00		8.27E+08	1.00E-05	3.07E-05	8.90E-01	E2
1	101	6.35E+00		5.61E+07	1.02E-06	3.10E-06	9.40E-01	E2
1	102	6.34E+00		1.52E+08	2.75E-06	8.34E-06	9.70E-01	E2
1	104	6.34E+00		2.21E+09	2.66E-05	8.05E-05	9.60E-01	E2
1	106	6.32E+00		1.13E+10	1.35E-04	4.08E-04	9.60E-01	E2
1	107	6.32E+00		1.59E+10	2.85E-04	8.54E-04	9.60E-01	E2
1	109	6.28E+00		6.24E+08	7.39E-06	2.18E-05	9.60E-01	E2
1	113	6.27E+00		6.12E+09	1.08E-04	3.17E-04	9.60E-01	E2
1	119	6.25E+00		5.96E+09	6.98E-05	2.03E-04	9.70E-01	E2
1	120	6.24E+00		6.05E+07	1.06E-06	3.08E-06	8.30E-01	E2
1	3	6.25E+01		1.24E+04	1.45E-08	3.17E+00		M2
1	6	2.33E+01		1.40E-01	3.40E-14	3.83E-07		M2
1	10	1.17E+01	11.675	1.81E+06	7.41E-08	1.05E-01		M2
1	13	1.02E+01		5.01E+00	2.34E-13	2.22E-07		M2
1	19	8.24E+00		2.64E+06	5.38E-08	2.70E-02		M2
1	23	7.81E+00		1.23E+01	3.38E-13	1.44E-07		M2
1	28	7.61E+00		2.59E+06	6.74E-08	2.65E-02		M2
1	30	7.57E+00		2.02E+06	5.21E-08	2.02E-02		M2
1	31	7.57E+00		3.55E+06	6.09E-08	2.36E-02		M2
1	32	7.31E+00	7.295	1.18E+05	1.89E-09	6.62E-04		M2
1	33	7.28E+00		1.86E+05	4.44E-09	1.53E-03		M2
1	34	7.27E+00	7.262	1.72E+04	2.72E-10	9.38E-05		M2
1	38	7.15E+00		1.09E+07	2.50E-07	8.16E-02		M2
1	39	7.15E+00	7.137	8.67E+06	1.33E-07	4.34E-02		M2
1	44	7.08E+00	7.077	9.27E+06	1.40E-07	4.44E-02		M2
1	46	7.07E+00		2.91E+06	6.54E-08	2.07E-02		M2
1	47	7.05E+00		2.30E+06	3.42E-08	1.07E-02		M2
1	51	6.89E+00	6.884	1.13E+04	1.61E-10	4.72E-05		M2
1	53	6.89E+00		2.34E+04	4.98E-10	1.46E-04		M2
1	55	6.85E+00		3.15E+00	6.64E-14	1.91E-08		M2
1	58	6.83E+00		2.88E+02	6.03E-12	1.71E-06		M2
1	110	6.27E+00		6.56E+04	7.73E-10	1.71E-04		M2
1	114	6.26E+00		8.64E+03	1.52E-10	3.34E-05		M2

h — Ref. [34]

In Table 4, we have also compared our transition wavelength calculated from MCDF method with the wavelength in the NIST database. One can see that maximum discrepancy between our MCDF and NIST results is 0.2%. Therefore, the difference between these results is not considerable. In Table 5, we have compared transitions wavelength with the other available experimental measured wavelength or theoretical calculations [45–49] which is also shown in Figure 1. Utter *et al*. [45] recorded extreme ultraviolet spectra of tungsten in the wavelength range 40-85 Å at the Livermore electron-beam ion-trap facility. There [45] measured wavelength for the transition 1-3 was 62.335 Å. Our theoretical results agree well with the experimental wavelengths and also with the theoretical wavelengths.

Table 5. Comparison of computed wavelengths (in Å) from GRASP with different theories and observed wavelengths for transitions from $3P^6 3D^{10} 4S\ ^2S_{1/2}$ to selected upper levels

Transition No.	Transitions	GRASP	OTHERS
1	1-3	62.5	62.334[a]
			62.304[b]
			62.334[c]
			62.335[d]
			62.341[e]
2	1-59	6.82	6.824[f]
3	1-51	6.89	6.893[f]
4	1-44	7.08	7.077[f]
5	1-41	7.14	7.138[f]
6	1-34	7.27	7.262[f]

[a] – Ref. [45]

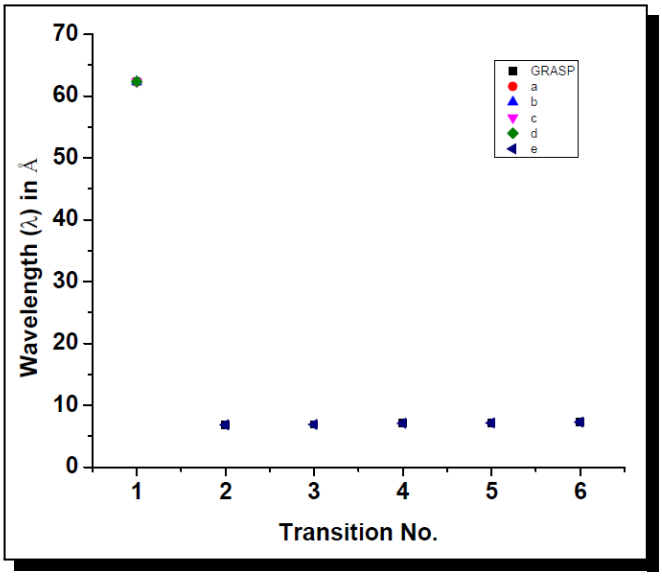

Figure 1. Wavelength comparison with reference [45–49]

4. Conclusion

Motivated by the need of data for fusion plasma, in the present paper, we have reported complete and reliable atomic data such as energy levels, radiative rates and lifetimes for E1, E2, M1 and M2 transitions for lowest 120 fine structure levels Cu-like W. In our calculations, both GRASP and FAC codes are implemented and the discrepancy in results of two independent codes is discussed. The effect of configuration interaction by including relativistic correction has been examined and investigates systematically. We found our results match well with NIST and other available results

Acknowledgments

Authors are thankful to Principal, Shyamlal College, University of Delhi for providing facilities and infrastructure for carrying out this work.

Competing Interests

The authors declare that they have no competing interests.

Authors' Contributions

All the authors contributed significantly in writing this article. The authors read and approved the final manuscript.

References

[1] C. H. Skinner, Atomic physics in the quest for fusion energy and ITER, *Physica Scripta* **T134** (2009), 014022, DOI: 10.1088/0031-8949/2009/T134/014022.

[2] R. Neu, K. B. Fournier, D. Schlögl and J. Rice, Observations of x-ray spectra from highly charged tungsten ions in tokamak plasmas, *Journal of Physics B: Atomic, Molecular and Optical Physics* **30** (1997), 5057, DOI: 10.1088/0953-4075/30/21/036.

[3] J. F. Seely, C. M. Brown and U. Feldman, Wavelengths and energy levels for the Cu I isoelectronic sequence Ru^{15+} through U^{63+}, *Atomic Data and Nuclear Data Tables* **43** (1989), 145, DOI: 10.1016/0092-640X(89)90017-X.

[4] C. M. Brown, J. F. Seely, D. R. Kania, B. A. Hammel, C. A. Back, R. W. Lee, A. Barshalom and W. E. Behring, Wavelengths and energy levels for the Zn I isoelectronic sequence Sn^{20+} through U^{62+}, *Atomic Data and Nuclear Data Tables* **58** (1994), 203, DOI: 10.1006/adnd.1994.1027.

[5] H. Hensberge, J. van Santvoort, K.A. van der Hucht and T. H. Morgan, The mid ultraviolet spectrum of α-2 CVn=HD 112413=HR4915, *Astronomy and Astrophysics* **158** (1986), 113.

[6] J. Clementson, P. Beiersdorfer, E. W. Magee, H. S. McLean and R. D. Wood, Tungsten spectroscopy relevant to the diagnostics of ITER divertor plasmas, *Journal of Physics B: Atomic, Molecular and Optical Physics* **43** (2010), 144009, DOI: 10.1088/0953-4075/43/14/144009.

[7] E. J. Doyle, W. A. Houlberg, Y. Kamada, V. Mukhovatov, T. H. Osborne, A. Polevoi, G. Bateman, J. W. Connor, J. G. Cordey, T. Fujita, X. Garbet, T. S. Hahm, L. D. Horton, A. E. Hubbard, F. Imbeaux, F. Jenko, J. E. Kinsey, Y. Kishimoto, J. Li, T. C. Luce, Y. Martin, M. Ossipenko, V. Parail, A. Peeters, T. L. Rhodes, J. E. Rice, C. M. Roach, V. Rozhansky, F. Ryter, G. Saibene, R. Sartori, A. C. C. Sips, J. A. Snipes, M. Sugihara, E. J. Synakowski, H. Takenaga, T. Takizuka, K. Thomsen, M. R. Wade, H. R. Wilson, ITPA Transport Physics Topical Group, ITPA Confinement Database and Modelling Topical Group and ITPA Pedestal and Edge Topical Group, Plasma confinement and transport (Chapter 2), *Nuclear Fusion* **47** (2007), 518, DOI: 10.1088/0029-5515/47/6/S02.

[8] R. Radtke, C. Biedermann, J. L. Schwob, P. Mandelbaum and R. Doron, Line and band emission from tungsten ions with charge 21+ to 45+ in the 45–70–Å range, *Physical Review A* **64** (2001), 012720, DOI: 10.1103/PhysRevA.64.012720.

[9] V. Jonauskas, S. Kučas and R. Karazija , On the interpretation of the intense emission of tungsten ions at about 5 nm, *Journal of Physics B: Atomic, Molecular and Optical Physics* **40** (2007), 2179, DOI: 10.1088/0953-4075/40/11/018.

[10] V. Jonauskas, R. Kisielius, A. Kynienė, S. Kučas and P. H. Norrington, Magnetic dipole transitions in $4d^N$ configurations of tungsten ions, *Physical Review A* **81** (2010), 012506, DOI: 10.1103/PhysRevA.81.012506.

[11] C. S. Harte, C. Suzuki, T. Kato, H. A. Sakaue, D. Kato, K. Sato, N. Tamura, S. Sudo, R. D'Arcy, E. Sokell, J. White and G. O'Sullivan, Tungsten spectra recorded at the LHD and comparison with calculations, *Journal of Physics B: Atomic, Molecular and Optical Physics* **43** (2010), 205004, DOI: 10.1088/0953-4075/43/20/205004.

[12] J. Clemetson and P. Beiersdorfer, Wavelength measurement of $n = 3$ to $n = 3$ transitions in highly charged tungsten ions, *Physical Review A* **81** (2010), 052509, DOI: 10.1103/PhysRevA.81.052509.

[13] Z. Fei, R. Zhao, Z. Shi, J. Xiao, M. Qiu, J. Grumer, M. Andersson, T. Brage, R. Hutton and Y. Zou, Experimental and theoretical study of the ground-state M1 transition in Ag-like tungsten, *Physical Review A* **86** (2012), 062501, DOI: 10.1103/PhysRevA.86.062501.

[14] P. Beiersdorfer, J. K. Lepson, M. B. Schneider and M. P. Bode, L-shell x-ray emission from neonlike W^{64+}, *Physical Review A* **86** (2012), 012509, DOI: 10.1103/PhysRevA.86.012509.

[15] Yu Ralchenko, I. N. Draganic, J. N. Tan, J. D. Gillaspy, J. M. Pomeroy, J. Reader, U. Feldman and G. E. Holland, EUV spectra of highly-charged ions W^{54+}–W^{63+} relevant to ITER diagnostics, *Journal of Physics B: Atomic, Molecular and Optical Physics* **41** (2008), 021003, DOI: 10.1088/0953-4075/41/2/021003.

[16] T. Pütterich, R. Neu, R. Dux, A. D. Whiteford, M. G. O'Mullane and the ASDEX Upgrade Team, Modelling of measured tungsten spectra from ASDEX/Upgrade and predictions for ITER, *Plasma Physics and Controlled Fusion* **50** (2008), 085016, DOI: 10.1088/0741-3335/50/8/085016.

[17] K. B. Fournier, Atomic data and spectral line intensities for highly ionized tungsten (Co-like W^{47+} to Rb-like W^{37+}) in a high temperature, low density plasma, *Atomic Data and Nuclear Data Tables* **68** (1998), 1, DOI: 10.1006/adnd.1997.0756.

[18] A. E. Kramida and T. Shirai, Energy levels and spectral lines of tungsten, W III through W LXXIV, *Atomic Data and Nuclear Data Tables* **95** (2009), 305 – 474, DOI: 10.1016/j.adt.2008.12.002.

[19] J. Clementson, P. Beiersdorfer, T. Brage and M. F. Gu, Atomic data and theoretical X-ray spectra of Ge-like through V-like W ions, *Atomic Data and Nuclear Data Tables* **100** (2014), 577, DOI: 10.1016/j.adt.2013.07.002.

[20] J. E. Sansonetti and J. J. Curry, Wavelengths, transition probabilities, and energy levels for the spectra of Barium (BaIII through BaLVI), *Journal of Physical and Chemical Reference Data* **39** (2010), 043103, DOI: 10.1063/1.3432516.

[21] C. Suzuki, F. Koike, I. Murakami, N. Tamura and S. Sudo, Observation of EUV spectra from gadolinium and neodymium ions in the large Helical device, *Journal of Physics B: Atomic, Molecular and Optical Physics* **45** (2012), 135002, DOI: 10.1088/0953-4075/45/13/135002.

[22] D. Kilbane, G. O'Sullivan, J. D. Gillaspy, Yu. Ralchenko and J. Reader, EUV spectra of Rb-like to Cu-like gadolinium ions in an electron-beam ion trap, *Physical Review A* **86** (2012), 042503, DOI: 10.1103/PhysRevA.86.042503.

[23] A. Goyal, I. Khatri, N. Singh, A. K. Singh, R. Sharma and M. Mohan, Atomic structure calculations and study of EUV and SXR spectral lines in Cu-like ions, *Canadian Journal of Physics* **94** (2016), 839, DOI: 10.1139/cjp-2016-0168.

[24] M. Xu, G. Jiang, M. Wu, X. Li, G. Bian and F. Hud, Multiconfiguration Dirac-Fock calculations of excitation energies and wavelengths in highly charged tungsten ions, *Canadian Journal of Physics* **94** (2016), 563, DOI: 10.1139/cjp-2015-0772.

[25] M. Klapisch, P. Mandelbaum, A. Barshalom, J. L. Schwob, A. Zigler and S. Jackel, Identification of $3d$–$4p$ transitions in Co-like W xlvii and Tm xliii and in Cu-like W xlvi and Tm xli from laser-produced plasmas, *Journal of the Optical Society of America* **71** (1981), 1276 – 1281, DOI: 10.1364/JOSA.71.001276.

[26] P. Mandelbaum, M. Klapisch, A. Bar-Shalom, J. L. Schwob and A. Zigler, Classification of x-ray spectra from laser produced plasmas of atoms from Tm to Pt in the range 6-9 Å, *Physica Scripta* **27** (1983), 39, DOI: 10.1088/0031-8949/27/1/005.

[27] M. Klapisch, P. Mandelbaum, A. Zigler, C. Bauche-Arnoult and J. Bauche, The unresolved $3d - 4f$ transitions in the x-ray spectra of highly ionized Tm to Re from laser produced plasma, *Physica Scripta* **34** (1986), 51, DOI: 10.1088/0031-8949/34/1/009.

[28] A. Zigler, J. Kolbe and R. W. Lee, Use of multilayer targets to inject trace elements into laser-produced plasma, *Applied Physics Letters* **50**, (1987), 1133, DOI: 10.1063/1.97939.

[29] J. Rzadkiewicz, Y. Yang, K. Kozioł, M. G. O'Mullane, A. Patel, J. Xiao, K. Yao, Y. Shen, D. Lu, R. Hutton, Y. Zou and JET Contributors, High-resolution tungsten spectroscopy relevant to the diagnostic of high-temperature tokamak plasmas, *Physical Review A* **97** (2018), 052501, DOI: 10.1103/PhysRevA.97.052501.

[30] G. C. Osborne, A. S. Safronova, V. L. Kantsyrev, U. I. Safronova, P. Beiersdorfer, K. M. Williamson, M. E. Weller and I. Shresthaa, Spectroscopic analysis and modeling of tungsten EBIT and Z-pinch plasma experiments, *Canadian Journal of Physics* **89** (2011), 599, DOI: 10.1139/p11-026.

[31] J. Clementson, P. Beiersdorfer, G. V. Brown and M. F. Gu, Spectroscopy of M-shell x-ray transitions in Zn-like through Co-like W, *Physica Scripta* **81** (2010), 015301, DOI: 10.1088/0031-8949/81/01/015301.

[32] Yu Ralchenko, J. Reader, J. M. Pomeroy, J. N. Tan and J. D. Gillaspy, Spectra of W^{39+}–W^{47+} in the 12-20 nm region observed with an EBIT light source, *Journal of Physics B: Atomic, Molecular and Optical Physics* **40** (2007), 3861, DOI: 10.1088/0953-4075/40/19/007.

[33] P. Palmeri, P. Quinet, É. Biémont and E. Träbert, Wavelengths and transition probabilities in heavy Ge-like ions ($70 \leq Z \leq 92$), *Atomic Data and Nuclear Data Tables* **93** (2007), 355 – 374, DOI: 10.1016/j.adt.2006.11.001.

[34] U. I. Safronova, A. S. Safronova and P. Beiersdorfer, Relativistic atomic data for Cu-like tungsten, *Physical Review A* **86** (2012), 042510, DOI: 10.1103/PhysRevA.86.042510.

[35] K. Kozioł and J. Rzadkiewicz, Multiconfiguration Dirac-Hartree-Fock and configuration- interaction study of $4d-3p$ x-ray transitions in Cu- and Ni-like tungsten ions, *Physical Review A* **98** (2018), 062504, DOI: 10.1103/PhysRevA.98.062504.

[36] I. P. Grant, B. J. Mckenzie, P. H. Norrington, D. F. Mayers and N. C. Pyper, An atomic multiconfigurational Dirac-Fock package, *Computer Physics Communications* **21** (1980), 207 – 231, DOI: 10.1016/0010-4655(80)90041-7.

[37] P. H. Norrington (2009), `http://www.am.qub.ac.uk/DARC/`.

[38] N. Singh, S. Aggarwal and M. Mohan, Theoretical study of energy levels and radiative properties of Be-like W^{70+}, *Journal of Electron Spectroscopy and Related Phenomena* **229** (2018), 124 – 131, DOI: 10.1016/j.elspec.2018.10.005.

[39] S. Aggarwal, J. Singh and M. Mohan, Breit–Pauli atomic structure calculations for Fe XI, *Atomic Data and Nuclear Data Tables* **99** (2013), 704 – 732, DOI: 10.1016/j.adt.2013.02.001.

[40] C. Kaur, S. Chaurasia, N. Singh, J. Pasley, S. Aggarwal and M. Mohan, L-shell spectroscopy of neon and fluorine like copper ions from laser produced plasma *Physics of Plasmas* **26** (2019), 023301, DOI: 10.1063/1.5051758.

[41] M. Mohan, S. Aggarwal and N. Singh, Multiconfigurational Dirac–Fock atomic structure calculations for Cl-like tungsten, *Canadian Journal of Physics* **92** (2014), 177, DOI: 10.1139/cjp-2013-0348.

[42] S. Aggarwal, J. Singh, A. K. S. Jha and M. Mohan, Energy levels and radiative transition rates for Ge XXXI, As XXXII, and Se XXXIII, *Atomic Data and Nuclear Data Tables* **100** (2014), 859 – 985, DOI: 10.1016/j.adt.2013.11.005.

[43] S. Aggarwal, A. K. Singh and M. Mohan, Atomic data for He-like tungsten, *Journal of Atomic, Molecular, Condensate and Nano Physics* **1** (2014), 19 – 30, DOI: 10.26713/jamcnp.v1i1.225.

[44] M. H. Cheng, K. T. Cheng and W. R. Johnson, Large-scale relativistic configuration-interaction calculation of the $2s^2 {}^1S_0$–$2s2p^3 P_1$ intercombination transition in C III, *Physical Review A* **64** (2001), 042507, DOI: 10.1103/PhysRevA.64.042507.

[45] S. B. Utter, P. Beiersdorfer and E. Träbert, Electron-beam ion-trap spectra of tungsten in the EUV, *Canadian Journal of Physics* **80**, 1503 – 1515, DOI: 10.1139/p02-132.

[46] J. F. Seely, C. M. Brown and W. E. Behring, Transitions in Fe-, Co-, Cu-, and Zn-like ions of W and Re, *Journal of the Optical Society of America B* **6** (1989), 3 – 6, DOI: 10.1364/JOSAB.6.000003.

[47] Y.-K. Kim, D. H. Baik, P. Indelicato and J. P. Desclaux, Resonance transition energies of Li-, Na-, and Cu-like ions, *Physical Review A* **44** (1991), 148, DOI: 10.1103/PhysRevA.44.148.

[48] S. B. Utter, P. Beiersdorfer, E. Träbert and E. J. Clthiaux, Wavelengths of the $4s_{1/2}-4p_{3/2}$ resonance lines in Cu-like heavy ions, *Physical Review A* **67** (2003), 032502, DOI: 10.1103/PhysRevA.67.032502.

[49] S. A. Blundell, Calculations of the screened self-energy and vacuum polarization in Li-like, Na-like, and Cu-like ions, *Physical Review A* **47** (1993), 1790, DOI: 10.1103/PhysRevA.47.1790.